

Effective vertex of quark production in collision of a Reggeized quark and gluon

M. G. Kozlov* and A. V. Reznichenko†

*Budker Institute of Nuclear Physics of Siberian Branch Russian Academy of Sciences,
Novosibirsk 630090, Russia and Novosibirsk State University, Novosibirsk 630090, Russia*

(Received 16 October 2015; published 21 December 2015)

We calculate the effective vertex of the quark production in the collision of a Reggeized quark and a Reggeized gluon in the next-to-leading order (NLO). The vertex in question is the missing component of the multi-Regge NLO amplitudes with the quark and gluon exchanges in the t_i channels. This multi-Regge form of the amplitudes is the important hypothesis which was recently proved for the gluon exchanges only and remains unverified within the next-to-leading-logarithmic approximation (NLA) for the general case including the quark exchanges. Our calculation allows one to develop the bootstrap approach to the quark Reggeization proof in NLA.

DOI: 10.1103/PhysRevD.92.125023

PACS numbers: 12.38.-t, 11.55.Jy, 12.38.Bx

I. INTRODUCTION

It is common knowledge that the multi-Regge form of amplitudes at high energies is a base of various theoretical constructions in quantum chromodynamics (QCD) and supersymmetric Yang-Mills theories (SYM). The most famous application of the form resulted in the Balitsky-Fadin-Kuraev-Lipatov (BFKL) [1–4] approach to the semi-hard processes description in QCD. The simplicity of the multi-Regge form was recently used as a powerful tool to test various factorization formulas in SYM, QCD, and in other gauge theories.

Let us now recall the state of the art for the Reggeization hypothesis proof. In QCD, the gluon Reggeization hypothesis (i.e., the multi-Regge form with only gluon exchanges in all t_i channels) was proved in the leading-logarithmic approximation (LLA) by the authors of the BFKL approach roughly 40 years ago. The analyticity and t -channel unitarity were the principal tools of this proof [5]. It proved to be a strong base for the BFKL approach in the leading approximation.

In the next-to-leading-logarithmic approximation (NLA) we developed the general method based on the compatibility of the hypothetical multi-Regge form of the amplitude with s -channel unitarity [6]. The compatibility is formulated as a series of so-called bootstrap relations, the fulfillment of which ensures the validity of the multi-Regge form order by order. The same method turned out to be fruitful in the proof of the multi-Regge form with the quark exchanges in LLA [7]. Then we used the bootstrap approach to prove the NLA gluon Reggeization hypothesis in QCD. The calculation of the quark and gluon one-loop corrections to all bootstrap components gave us the possibility to verify all bootstrap relations [8–11]. Once

again our general method was successfully applied to prove NLA gluon Reggeization within SYM theories with arbitrary \mathcal{N} and in the theories with a general form of the Yukawa interaction [12]. Theoretically our bootstrap approach is applicable for the quark Reggeization NLA proof. But the only unknown component of the NLA amplitude is the Reggeon(G)-Reggeon(Q)-quark one-loop vertex $\gamma_{G_1 Q_2}^Q$.

The only missing link of the recurrent bootstrap procedure is the “initial condition.” For NLA it is the one-loop amplitude with arbitrary leg number n . We supposed that these amplitudes have the correct factorized form corresponding to the multi-Regge ansatz. It has been verified for small n but should be proved in general.

The main goal of our investigation is to complete the quark Reggeization hypothesis formulation in NLA. For this purpose one should know all effective Reggeon vertices appearing in the multi-Regge form with the quark exchanges up to next-to-leading order. The vertex $\gamma_{G_1 Q_2}^Q$ in next-to-leading order (NLO) is the final uncalculated component of the amplitude. Another aspect of interest is the construction of the evolution equation kernel in NLO for the Reggeized quark. The vertex $\gamma_{G_1 Q_2}^Q$ is the final ingredient for the kernel construction. The kernel is of concern since its conformal properties in SYM theory can illuminate the integrability property of this theory and give the connection between different approaches as it occurred for the gluon NLO kernel. Finally, there are some processes (for instance, recharging processes $p + p \rightarrow n + \Delta^{++}$, $p + \bar{p} \rightarrow n + \bar{n}$ with u - and d -quark exchanges) where the quark exchange amplitude (subleading in comparison with the gluon one) might dominantly contribute. Our Reggeon vertices are of some phenomenological interest for these processes.

The article is organized as follows. The second section is devoted to an explanation of our method of calculation and

*M.G.Kozlov@inp.nsk.su

†A.V.Reznichenko@inp.nsk.su

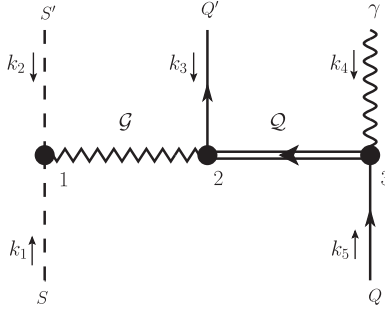


FIG. 1. Regge amplitude of the process $SQ \rightarrow S'Q'\gamma$ and Q are the Reggeized gluon in the t_1 channel and the Reggeized quark in the t_2 channel, respectively. Here blob 1 is the effective vertex $\Gamma_{S'S}^G$, blob 2 is the unknown vertex $\gamma_{GQ}^{Q'}$, and blob 3 is the vertex $\Gamma_{\gamma Q}^Q$.

to the description of kinematics. The third section presents the Reggeization hypothesis, components of the Regge amplitude, and Lorentz and color structures of our one-loop amplitude in the multi-Regge kinematics. In the fourth section we present the result of our calculation, both in fragmentation form (reproducing different components of our Regge amplitude) and as the full expression. At the end of the fourth section we present the resulting expression for the required vertex $\gamma_{G_1 Q_2}^Q$. In the Appendix we introduce the technique of the loop integration and give the explicit expressions for the master integrals of our calculation.

II. AMPLITUDE OF THE QUARK PRODUCTION IN MULTI-REGGE KINEMATICS

There are several steps to finding the NLO effective vertex $\gamma_{G_1 Q_2}^Q$ in the next-to-leading order. To calculate this Reggeon vertex we can consider any simple process with this vertex in the one-loop approximation. We choose the amplitude $SQ \rightarrow S'Q'\gamma$ of the scalar, quark, and photon production in the scalar and quark collision; see Fig. 1. It does not matter for the vertex calculation whether we analyze the amplitude in Yang-Mills theory with N_c gluons, the photon, n_f quarks (in the fundamental color representation), and n_s scalars (in the adjoint representation), or simply the QCD amplitude.

We first consider all one-loop Feynman diagrams contributing to the process $SQ \rightarrow S'Q'\gamma$. There are 23 different nontrivial one-loop Feynman diagrams; see Fig. 2. There are some diagrams labeled according to their class: pentagons, boxes, triangles, and bubble diagrams. First of all we perform the reduction of the amplitude to the master integrals using the ‘‘LiteRed’’[13] MATHEMATICA package. As a result of the reduction one has pentagon, box, and self-energy nontrivial master integrals. Our master integrals are listed in the Appendix. The method of our tensor integral calculation is presented in the Appendix as well. The algorithm of the master integral calculation is presented in

Ref. [14]. The next stage is to take the Regge limit of the resulting expression for the master integrals analytically continued in the physical kinematic region. Finally, we compare the result of our calculation with the one-loop expression resulting from the hypothetical multi-Regge form of the amplitude in question. In such a way we extract the required vertex.

A. Kinematics, color, and Lorentz structures of the amplitude

The momentum of the initial scalar S is k_1 , that of the final scalar S' is k_2 , that of the final quark Q' produced in the central rapidity region is k_3 , that of the final photon γ is k_4 , and that of the initial quark Q is k_5 . In Fig. 1 all momenta are considered to be incoming and light-cone: $k_1 + k_2 + k_3 + k_4 + k_5 = 0$, $k_i^2 = 0$. We use the physical gauge with a light-cone vector along k_1 for the final photon: $e(k_4) \cdot k_4 = 0$, $e(k_4) \cdot k_1 = 0$.

We present Sudakov’s decomposition for our momenta with the incoming scalar and quark momenta being along the light-cone momenta n_1 , n_2 ($n_1^2 = 0$, $n_2^2 = 0$, $n_1 \cdot n_2 = 1$): $k_1 = k_1^+ n_1$, $k_i = k_i^+ n_1 + k_i^- n_2 + k_{i\perp}$ for $i = 2, 3, 4$, and $k_5 = k_5^- n_2$. Here n_1, n_2 are light-cone momenta, where $k_i^\pm = k_i \cdot n_{2,1}$. Here and below the \perp sign is used for components of momenta transverse to the n_1, n_2 plane. The scalar products of particle momenta are expressed through Lorentz invariants,

$$\begin{aligned} s &= 2k_1 \cdot k_5, & t_1 &= 2k_1 \cdot k_2, \\ t_2 &= 2k_4 \cdot k_5, & s_1 &= 2k_2 \cdot k_3, & s_2 &= 2k_3 \cdot k_4, \\ u_1 &= 2k_1 \cdot k_3, & u_2 &= 2k_3 \cdot k_5, \\ u &= 2k_1 \cdot k_4, & s' &= 2k_2 \cdot k_4, & u' &= 2k_2 \cdot k_5. \end{aligned} \quad (2.1)$$

And we express the other invariants through an independent set: $u_1 = t_2 - t_1 - s_1, u_2 = t_1 - t_2 - s_2, u = s_1 - t_2 - s, s' = s - s_1 - s_2, u' = s_2 - t_1 - s$. It is important that independent invariants have the following signs in the physical region of our process: $s_1 > 0, s_2 > 0, s > 0, t_1 < 0, t_2 < 0$ (and $u_1 < 0, u_2 < 0, u < 0, s' > 0, u' < 0$).

The multi-Regge kinematics (MRK) means that we have particles well separated in rapidity space in the final state,

$$k_2^+ \gg k_3^+ \gg k_4^+, \quad k_2^- \ll k_3^- \ll k_4^-. \quad (2.2)$$

Since momenta k_i are on the mass shell one has $k_i^- = -\frac{k_{i\perp}^2}{2k_i^+}$, $i = 2, 3, 4$. We introduce two dimensionless large (in the Regge limit) parameters: $y_1 = k_2^+/k_3^+ \gg 1$ and $y_2 = k_3^+/k_4^+ \gg 1$. Hereinafter we will use dimensional regularization $D = 4 + 2\epsilon$ and we will take the limit $\epsilon \rightarrow 0$ before the Regge limit. MRK implies also that all transverse momenta are not increasing as $y_i \rightarrow \infty$. One can express all of the transverse scalar products through

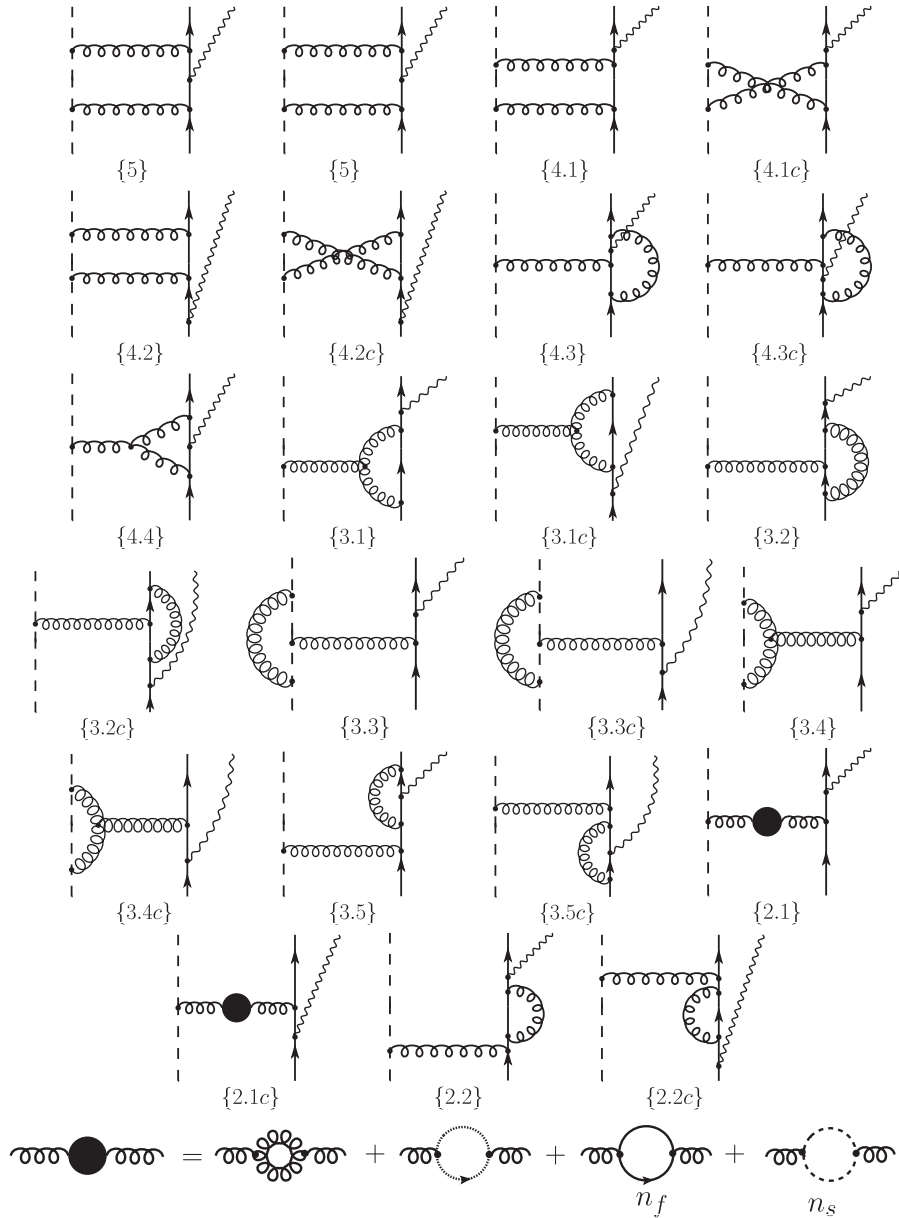


FIG. 2. Nontrivial one-loop diagrams for the process $SQ \rightarrow S'Q'\gamma$: pentagons (labeled as $\{5\}$ and crossed diagrams $\{5c\}$), boxes ($\{4.X\}$ and crossed diagrams $\{4.Xc\}$), triangles ($\{3.X\}$ and crossed diagrams $\{3.Xc\}$), and bubbles ($\{2.X\}$ and crossed diagrams $\{2.Xc\}$). The last line is the self-energy insertion with gluons, ghosts, n_f types of fermions, and n_s types of scalars.

independent ones: $(k_{2\perp}^2, k_{3\perp}^2, k_{4\perp}^2)$ $2(k_2 \cdot k_3)_\perp = k_{4\perp}^2 - k_{2\perp}^2 - k_{3\perp}^2$, $2(k_3 \cdot k_4)_\perp = k_{2\perp}^2 - k_{3\perp}^2 - k_{4\perp}^2$, and $2(k_2 \cdot k_4)_\perp = k_{3\perp}^2 - k_{2\perp}^2 - k_{4\perp}^2$.

Further, we consider the one-loop amplitude $SQ \rightarrow S'Q'\gamma$ as a power function of y_1, y_2 within the accuracy of logarithmic terms (i.e., terms $\ln^k[y_i]$ technically originating from the ϵ decomposition of master integrals). In the Regge limit the leading amplitude behavior is expected to be $\sim y_1 \sqrt{y_2}$. Here the factor y_1 comes from the Reggeized gluon in the s_1 channel and $\sqrt{y_2}$ comes from the Reggeized quark in the s_2 channel; see Fig. 1. Our basis bispinor structures (2.4) are proportional to $\sqrt{y_2}$, which is why the

order of the multi-Regge limit calculation for the amplitude is as follows: an expansion in $\epsilon \rightarrow 0$ with accuracy $\mathcal{O}(\epsilon)$, followed by retaining the leading asymptotic power expansion in $y_i \rightarrow \infty$.

There are only two independent color structures: the “tree” structure $T_{S'S}^a t^a$ and the “cross-box” structure $T_{S'C}^a T_{CS}^b t^b t^a$. Here t^a are $SU(N_c)$ quark generators in the fundamental representation, and $T_{S'S}^a = -if^{aS'S}$ are generators of scalars in the adjoint representation. The “tree” structure (i.e., color octet in the t_1 channel) turns out to give the leading contribution to the real part of our amplitude. Next, we use the following notation for the Casimir operator:

$$t^a t^a = C_F = \frac{N_c^2 - 1}{2N_c}. \quad (2.3)$$

The amplitude depends not only on the invariants of s_1, s_2, t_1, t_2, s , but on the helicity states of the external particles as well.

We assume that external momenta k_i are embedded in a four-dimensional subspace of the momentum space with $D = 4 + 2\epsilon$ dimensions, while the photon polarization is a D -vector. There are six independent Lorentz helicity structures in that case:

$$\begin{aligned} & \bar{u}(k_3) \not{\epsilon} u(k_5), & \bar{u}(k_3) \not{K}_1 \not{K}_4 \not{\epsilon} u(k_5), \\ & (e \cdot k_2) \bar{u}(k_3) \not{K}_1 u(k_5), & (e \cdot k_2) \bar{u}(k_3) \not{K}_4 u(k_5), \\ & (e \cdot k_3) \bar{u}(k_3) \not{K}_1 u(k_5), & (e \cdot k_3) \bar{u}(k_3) \not{K}_4 u(k_5). \end{aligned} \quad (2.4)$$

In the multi-Regge kinematics we can choose the following independent structures with only transverse ($D - 2$) components involved:

$$\begin{aligned} & \bar{u}(k_3) \not{\epsilon}_\perp u(k_5), & \bar{u}(k_3) \not{K}_{2\perp} \not{K}_{4\perp} \not{\epsilon}_\perp u(k_5), \\ & (e \cdot k_2)_\perp \bar{u}(k_3) \not{K}_{2\perp} u(k_5), & (e \cdot k_2)_\perp \bar{u}(k_3) \not{K}_{4\perp} u(k_5), \\ & (e \cdot k_4)_\perp \bar{u}(k_3) \not{K}_{2\perp} u(k_5), & (e \cdot k_4)_\perp \bar{u}(k_3) \not{K}_{4\perp} u(k_5). \end{aligned} \quad (2.5)$$

In the limit $D \rightarrow 4$ the first two structures become dependent since one can express $\not{\epsilon}_\perp$ in terms of $\not{K}_{2\perp}, \not{K}_{4\perp}$,

$$\begin{aligned} \not{\epsilon}_\perp^\mu &= k_{2\perp}^\mu \frac{k_{4\perp}^2 (e \cdot k_2)_\perp - (k_2 \cdot k_4)_\perp (e \cdot k_4)_\perp}{k_{2\perp}^2 k_{4\perp}^2 - (k_2 \cdot k_4)_\perp^2} \\ &+ k_{4\perp}^\mu \frac{-(k_2 \cdot k_4)_\perp (e \cdot k_2)_\perp + k_{2\perp}^2 (e \cdot k_4)_\perp}{k_{2\perp}^2 k_{4\perp}^2 - (k_2 \cdot k_4)_\perp^2}. \end{aligned} \quad (2.6)$$

This means that the part of the metric tensor $g_{D-4}^{\mu\nu} \sim \mathcal{O}(\epsilon)$ vanishes in the dimensional limit $D \rightarrow 4$.

III. REGGE AMPLITUDE STRUCTURE

According to the hypothesis of the quark and gluon Reggeization in NLA the real part of the amplitude $A + B \rightarrow A' + J_1 + \dots + J_n + B'$ in the MRK has the form

$$\begin{aligned} \Re \mathcal{A}_{2 \rightarrow n+2} &= \bar{\Gamma}_{A'A}^{R_1} \left(\mathcal{P} \prod_{i=1}^n e^{\omega_{R_i}(q_i)(z_{i-1} - z_i)} \hat{D}_{R_i} \gamma_{R_i R_{i+1}}^{J_i} \right) \\ &\times e^{\omega_{R_{n+1}}(q_{n+1})(z_n - z_{n+1})} \hat{D}_{R_{n+1}} \Gamma_{B'B}^{R_{n+1}}, \end{aligned} \quad (3.1)$$

where $\mathcal{P} \prod$ is the product ordered along the fermion line. We use the notation

$$\hat{D}_{R_i} = \begin{cases} \frac{1}{q_{i\perp}^2}, & R_i = \mathcal{G}_i, \\ -\frac{q_{i\perp}}{q_{i\perp}^3}, & R_i = \mathcal{Q}_i \end{cases} \quad (3.2)$$

for the Reggeon R_i (gluon or quark) propagator. Then $z_i = \frac{1}{2} \ln \frac{k_i^+}{k_i^-}$ are rapidities of the final jets J_i . In NLA, jets J_i are either one parton or the partons couple with close rapidities. Last, $\omega_R(q)$ in Eq. (3.1) is the Regge trajectory of the Reggeon R (gluon or quark) with momentum q .

There are several effective vertices ($\bar{\Gamma}_{A'A}^{R_1}, \Gamma_{B'B}^{R_{n+1}}$) for the particle-jet transition in the ‘‘fragmentation’’ kinematic region. As for the particle-particle transition (pure multi-Regge kinematics) one has the following vertices in QCD:

$$\Gamma_{G'G}^G, \quad \Gamma_{Q'Q}^G, \quad \Gamma_{G'Q}^Q.$$

There is an extra vertex $\Gamma_{S'S}^G$ for SYM. All these vertices are calculated within the NLO [15] (for the SYM case see Ref. [12]). The vertex of the quark-photon transition $\Gamma_{\gamma'Q}^Q$ may be found in Ref. [15] as well. For the quasi-multi-Regge kinematics (QMRK) case of the particle-couple transition one has

$$\begin{aligned} & \Gamma_{\{G_1 G_2\}G}^G, & \Gamma_{\{Q_1 Q_2\}G}^G, & \Gamma_{\{G_1 Q_2\}Q}^G, \\ & \Gamma_{\{G_1 G_2\}Q}^Q, & \Gamma_{\{G_1 Q_2\}G}^Q, & \Gamma_{\{Q_1 Q_2\}Q}^Q \end{aligned}$$

in QCD. All these vertices are known; see Refs. [16,17]. For SYM there are some additional vertices ($\Gamma_{\{S_1 S_2\}G}^G, \Gamma_{\{G'S\}S}^G, \Gamma_{\{Q_1 Q_2\}S}^G, \Gamma_{\{Q'S\}Q}^G$): the corresponding calculation can be found in Ref. [12].

There are several effective vertices ($\gamma_{R_i R_{i+1}}^{J_i}$) for the jet production in the Reggeon-Reggeon collision in the central region of rapidity. For one-particle production we have the QCD vertices

$$\gamma_{G_1 G_2}^G, \quad \gamma_{Q_1 Q_2}^G, \quad \gamma_{Q_1 G_2}^Q.$$

The vertices $\gamma_{G_1 G_2}^G, \gamma_{Q_1 Q_2}^G$ were calculated in NLO [18–21]. The effective vertex $\gamma_{Q_1 G_2}^Q$ was calculated in the leading order only. Our purpose is to find one-loop corrections to it. Vertices for couple production (QMRK) in the central region of rapidity

$$\begin{aligned} & \gamma_{G_1 G_2}^{\{G_1 G_2\}}, & \gamma_{G_1 G_2}^{\{Q_1 Q_2\}}, & \gamma_{Q_1 G_2}^{\{Q_1 G_2\}}, \\ & \gamma_{Q_1 Q_2}^{\{G_1 G_2\}}, & \gamma_{Q_1 Q_2}^{\{Q_1 Q_2\}} \end{aligned}$$

are calculated in QCD with required NLO accuracy [16,17] as well. In SYM one has an extra vertex, $\gamma_{R_1 R_2}^{\{S_1 S_2\}}$, which was calculated some years ago [22].

Note that QMRK is “subleading” kinematic, i.e., all necessary vertices should be taken at the tree level. The Reggeization hypothesis was proved in Ref. [23] for QMRK amplitudes with quark (and gluon) exchanges.

In the following we will use the standard momentum notations for the Regge amplitude $SQ \rightarrow S'Q'\gamma$ (see Fig. 1),

$$\begin{aligned} q_{1\perp} &\equiv (k_2 + k_1)_\perp = k_{2\perp}, \\ q_{2\perp} &\equiv (-k_4 - k_5)_\perp = -k_{4\perp}, \\ k_\perp &\equiv -k_{3\perp}, \end{aligned} \quad (3.3)$$

with k being the momentum of the quark produced. According to the hypothesis of the quark and gluon Reggeization in NLA [Eq. (3.1)], the real part of the amplitude $SQ \rightarrow S'Q'\gamma$ in the multi-Regge kinematics reads

$$\begin{aligned} \Re \mathcal{A}_8 &= \Gamma_{S'S}^{R_1} \left(\frac{s_1}{\sqrt{q_{1\perp}^2 k_\perp^2}} \right)^{\omega_g(q_1)} \frac{1}{q_{1\perp}^2} \gamma_{R_1 Q_2}^Q \left(\frac{s_2}{\sqrt{k_\perp^2 q_{2\perp}^2}} \right)^{\omega_g(q_2)} \\ &\times \left[-\frac{q_{2\perp}}{q_{2\perp}^2} \right] \Gamma_{\gamma Q}^{Q_2}. \end{aligned} \quad (3.4)$$

A. Regge trajectories and effective vertices

Now we present an expression for the one-loop trajectories of a quark and gluon,

$$\begin{aligned} \omega_q(q) &= -2C_F g^2 (-ia_\Gamma) \frac{(-q_\perp^2)^\epsilon}{\epsilon}, \\ \omega_g(q) &= -2N_c g^2 (-ia_\Gamma) \frac{(-q_\perp^2)^\epsilon}{\epsilon}. \end{aligned} \quad (3.5)$$

The constant a_Γ emerges from the integrals as a common factor [Eq. (A8)]. The combination of $N_c g^2 (-ia_\Gamma)$ will arise often and it is related to the \bar{g}^2 notation as follows:

$$\begin{aligned} N_c g^2 (-ia_\Gamma) &\equiv N_c g^2 \frac{\Gamma(1-\epsilon) \Gamma^2(1+\epsilon)}{(4\pi)^{2+\epsilon} \Gamma(1+2\epsilon)} \\ &= \bar{g}^2 \left(1 - \frac{\pi^2}{6} \epsilon^2 + \mathcal{O}(\epsilon^3) \right). \end{aligned} \quad (3.6)$$

Now we present the scalar-to-scalar Regge vertex in the following way [12]:

$$\Gamma_{S'S}^{R_1} = 2k_1^+ g T_{S'S}^{R_1} (1 + \delta_S), \quad \delta_S = \delta_S^c + \delta_S^{s.e.} + \delta_S^v + \delta_S^A. \quad (3.7)$$

Expressions for the corrections (δ 's) to the vertex of the scalar scattering can be found in Ref. [12] (there are corrections in the framework of supersymmetric Yang-Mills theory, but the QCD result can be obtained easily),

$$\delta_S^A + \delta_S^c = (-ia_\Gamma) g^2 N_c (-q_{1\perp}^2)^\epsilon \left(-\frac{5}{4\epsilon^2} + \frac{1}{2\epsilon} - 1 + \frac{\pi^2}{2} \right), \quad (3.8)$$

$$\begin{aligned} \delta_S^{s.e.} &= (-ia_\Gamma) N_c g^2 \frac{(-q_{1\perp}^2)^\epsilon}{\epsilon} \left(-\left[\frac{5}{6} - \frac{31}{18} \epsilon \right] \right. \\ &\quad \left. + n_s \left[\frac{1}{12} - \frac{2}{9} \epsilon \right] + \frac{n_f}{N_c} \left[\frac{1}{3} - \frac{5}{9} \epsilon \right] \right), \end{aligned} \quad (3.9)$$

$$\begin{aligned} \delta_S^v &= (-ia_\Gamma) N_c g^2 \frac{(-q_{1\perp}^2)^\epsilon}{\epsilon^2} \left(\left[\frac{5}{4} - \frac{3}{2} \epsilon + 3\epsilon^2 \right] \right. \\ &\quad \left. + [-2 + 4\epsilon - 8\epsilon^2] \right). \end{aligned} \quad (3.10)$$

Here the superscript c denotes the universal contribution from the central rapidity region, the index $s.e.$ denotes the contribution of the mass (self-energy) operator, the index v denotes the contribution of the vertex corrections, and the index A represents the contribution coming from the rapidity close to the initial particle. All corrections are presented in the ϵ decomposition with the required accuracy.

Corrections to the vertex of photon production are more complicated since the structure contains helicity-violating terms:

$$\Gamma_{\gamma Q}^{Q_2} = -e \left(\not{\epsilon}_\perp + \not{\epsilon}_\perp \delta_{1\gamma} + \frac{(e \cdot q_2)_\perp}{q_{2\perp}^2} \not{q}_{2\perp} \delta_{2\gamma} \right) u(k_5), \quad (3.11)$$

$$\delta_{1\gamma} = \delta_{1\gamma}^{s.e.} + \delta_{1\gamma}^v + \delta_{1\gamma}^A + \delta_{1\gamma}^c, \quad \delta_{2\gamma} = \delta_{2\gamma}^v + \delta_{2\gamma}^A. \quad (3.12)$$

Expression for these corrections can be found in Ref. [15]:

$$\delta_{1\gamma}^A + \delta_{1\gamma}^c = g^2 (-ia_\Gamma) (-q_{2\perp}^2)^\epsilon (-C_F) \left[\frac{1}{\epsilon^2} - \frac{\pi^2}{2} \right], \quad (3.13)$$

$$\delta_{1\gamma}^v = C_F g^2 (-ia_\Gamma) (-q_{2\perp}^2)^\epsilon \frac{1-4\epsilon}{\epsilon}, \quad (3.14)$$

$$\delta_{1\gamma}^{s.e.} = C_F g^2 (-ia_\Gamma) (-q_{2\perp}^2)^\epsilon \frac{1-\epsilon}{2\epsilon}, \quad (3.15)$$

$$\delta_{2\gamma}^v = C_F g^2 (-ia_\Gamma) (-q_{2\perp}^2)^\epsilon \frac{(-2)(2-5\epsilon)}{\epsilon}, \quad (3.16)$$

$$\delta_{2\gamma}^A = C_F g^2 (-ia_\Gamma) (-q_{2\perp}^2)^\epsilon \frac{4(1-2\epsilon)}{\epsilon}. \quad (3.17)$$

We parametrize the unknown vertex of quark production in the quark-Reggeon collision as

$$\gamma_{R_1 Q_2}^Q = -g \frac{1}{k_3^+} \bar{u}(k_3) t^{R_1} (\not{q}_{1\perp} + \not{q}_{1\perp} \delta_{1Q} + \not{q}_{2\perp} \delta_{2Q}). \quad (3.18)$$

The term δ_{1Q} is a correction to the leading-order structure. The correction δ_{2Q} stands before the structure, which is absent in the leading order (the mass operator corrections contribute only in the δ_{1Q} coefficient),

$$\delta_{1Q} = \delta_{1Q}^{s.e.1} + \delta_{1Q}^{s.e.2} + \delta_{1Q}^{v.c}, \quad \delta_{2Q} = \delta_{2Q}^{v.c}. \quad (3.19)$$

B. Lorentz and color structures of the Regge amplitude

Now we consider the real part of the amplitude in question.

In the first place we will be interested in the octet color (or ‘‘tree’’) structure coefficient of the Regge amplitude obtained in our calculation after the Regge limit procedure.

Let us introduce the notation for the basic Lorentz structures of our Regge amplitude. There is only one Born structure,

$$A^{\text{Born}} = -2y_1 g^2 e T_{S'S}^{R_1} \frac{\bar{u}(k_3) t^{R_1} q_{1\perp} q_{2\perp} e_{\perp} u(k_5)}{q_{1\perp}^2 q_{2\perp}^2}. \quad (3.20)$$

The next structure A_8^e arises from the correction to the Regge vertex for quark production in the central region and violates the helicity,

$$A_8^e = -2y_1 g^2 e T_{S'S}^{R_1} \frac{\bar{u}(k_3) t^{R_1} e_{\perp} u(k_5)}{q_{1\perp}^2}. \quad (3.21)$$

The structure $A_8^{q_1}$ arises from the correction to the Regge vertex for the quark-photon transition and violates the helicity as well,

$$A_8^{q_1} = -2y_1 g^2 e T_{S'S}^{R_1} \frac{\bar{u}(k_3) t^{R_1} q_{1\perp} u(k_5) (e \cdot q_2)_{\perp}}{q_{1\perp}^2 q_{2\perp}^2}. \quad (3.22)$$

The final structure that appears after the Regge limit in our calculations is as follows:

$$A_8^{q_2} = -2y_1 g^2 e T_{S'S}^{R_1} \frac{\bar{u}(k_3) t^{R_1} q_{2\perp} u(k_5) (e \cdot q_2)_{\perp}}{q_{1\perp}^2 q_{2\perp}^2}. \quad (3.23)$$

The decomposition of the multi-Regge form of the amplitude $SQ \rightarrow S'Q'\gamma$ [Eq. (3.4)] in the coupling constant up to the next-to-leading order gives us

$$\begin{aligned} \Re \mathcal{A}_8 = & A^{\text{Born}} \left(1 + \omega_g(q_1) \ln y_1 + \omega_q(q_2) \ln y_2 \right. \\ & + \frac{\omega_g(q_1)}{2} \ln \left[\frac{k_{\perp}^2}{q_{1\perp}^2} \right] + \frac{\omega_q(q_2)}{2} \ln \left[\frac{q_{2\perp}^2}{k_{\perp}^2} \right] \\ & \left. + \delta_s + \delta_{1Q} + \delta_{1\gamma} \right) + A_8^e \delta_{2Q} + A_8^{q_1} \delta_{2\gamma} + \mathcal{O}(eg^6). \end{aligned} \quad (3.24)$$

If we calculate one-loop corrections for the amplitude $SQ \rightarrow S'Q'\gamma$ and take from the amplitude known corrections for the effective vertices $\Gamma_{S'S}^G, \Gamma_{\gamma Q}^Q$ and the terms with Regge trajectory contribution, then we obtain the corrections for the effective vertex γ_{GQ}^Q .

IV. RESULT OF THE AMPLITUDE $SQ \rightarrow S'Q'\gamma$ CALCULATION

Let us present the result of the calculation procedure described at the beginning of Sec. II. Here we give the calculation result in the Regge limit and group diagrams into the expressions with specific elements for the Regge amplitude. We use the notations (3.20)–(3.23) for structures from the previous section and the notation (A8) for the common factor a_{Γ} .

Now we present characteristic diagram contributions reproducing different components of the Regge amplitude: photon and scalar vertex corrections, Regge trajectories, and the corrections to the unknown vertex.

The sum of diagrams providing the corrections to the photon vertex reads

$$\begin{aligned} & \Re(A_{3.5} + A_{3.5c}) \\ & = g^2 (-ia_{\Gamma}) C_F \left\{ -A_8^e \ln y_2 - (-q_{2\perp}^2)^{\epsilon} \frac{1}{\epsilon} [2(2 - 5\epsilon)] \right. \\ & \quad \left. \times (A_8^{q_1} + A_8^{q_2}) - (1 - 4\epsilon) A^{\text{Born}} \right\}. \end{aligned} \quad (4.1)$$

It is easy to see that these diagrams (the 3.5 group) contain a large logarithm $\ln y_2$. Diagrams describing the mass operator of the quark in the t_2 channel contain $\ln y_2$ as well:

$$\begin{aligned} & \Re(A_{2.2} + A_{2.2c}) \\ & = g^2 (-ia_{\Gamma}) C_F \left(A^{\text{Born}} \frac{1 - \epsilon}{\epsilon} (-q_{2\perp}^2)^{\epsilon} - A_8^e \ln y_2 \right). \end{aligned} \quad (4.2)$$

Diagrams of the vacuum polarization of the gluon in the t_1 channel result in the expression (in the $\epsilon \rightarrow 0$ decomposition)

$$\begin{aligned} A_{2.1X} = & N_c g^2 (-ia_{\Gamma}) A^{\text{Born}} \frac{(-q_{1\perp}^2)^{\epsilon}}{\epsilon} \left(-\left(\frac{5}{3} - \frac{31}{9} \epsilon \right) \right. \\ & \left. + \frac{n_s}{2} \left(\frac{1}{3} - \frac{8}{9} \epsilon \right) + \frac{n_f}{N_c} \left(\frac{2}{3} - \frac{10}{9} \epsilon \right) \right). \end{aligned} \quad (4.3)$$

The following group of diagrams provides the correction to the scalar vertex:

$$\begin{aligned}
& A_{3.3} + A_{3.3c} + A_{3.4} + A_{3.4c} \\
&= N_c g^2 (-ia_T) A^{\text{Bom}} \frac{(-q_{1\perp}^2)^\epsilon}{\epsilon^2} \\
&\quad \times \left(-(2 - 4\epsilon + 8\epsilon^2) + \frac{1}{4}(5 - 6\epsilon + 12\epsilon^2) \right). \quad (4.4)
\end{aligned}$$

Diagrams describing the Reggeization of quarks and gluons (i.e., yielding the Regge trajectories) and delivering the correction to the vertex of the quark production in the central region give the following real part for the octet (tree) color structure:

$$\begin{aligned}
& \Re(A_5 + A_{4.1} + A_{4.2} + A_{4.3} + A_{4.3c} + A_{4.4} + A_{3.1} + A_{3.1c} + A_{3.2} + A_{3.2c})|_8 = -ig^2 a_T \\
&\quad \times \left\{ A_8^\epsilon \left[(N_c - C_F) \left(1 + \frac{k_\perp^2}{q_{1\perp}^2 - q_{2\perp}^2} - \frac{q_{1\perp}^2 k_\perp^2}{(q_{1\perp}^2 - q_{2\perp}^2)^2} \ln \left[\frac{q_{1\perp}^2}{q_{2\perp}^2} \right] \right) \right. \right. \\
&\quad + C_F \left(\frac{3q_{1\perp}^2}{q_{1\perp}^2 - q_{2\perp}^2} \ln \left[\frac{q_{1\perp}^2}{q_{2\perp}^2} \right] + 2 \ln y_2 \right) \left. \right] + A^{\text{Bom}} \left[C_F \left(-\frac{2-\epsilon}{\epsilon^2} (-q_{2\perp}^2)^\epsilon - \frac{2}{\epsilon} (-q_{2\perp}^2)^\epsilon \ln y_2 \right. \right. \\
&\quad + \frac{2\pi^2}{3} - 4 + \frac{3q_{1\perp}^2}{q_{1\perp}^2 - q_{2\perp}^2} \ln \left[\frac{q_{1\perp}^2}{q_{2\perp}^2} \right] + 2\text{Li}_2 \left[1 - \frac{q_{1\perp}^2}{q_{2\perp}^2} \right] \left. \right) - N_c \left(\frac{1}{\epsilon^2} (-k_\perp^2)^\epsilon + \frac{2}{\epsilon} (-q_{1\perp}^2)^\epsilon \ln y_1 \right. \\
&\quad + \frac{1+2\epsilon}{4\epsilon^2} (-q_{1\perp}^2)^\epsilon - \frac{2\pi^2}{3} - 2 + \ln \left[\frac{q_{1\perp}^2}{q_{2\perp}^2} \right] \ln \left[\frac{k_\perp^2}{q_{2\perp}^2} \right] + 2\text{Li}_2 \left[1 - \frac{q_{1\perp}^2}{q_{2\perp}^2} \right] \left. \right) \left. \right] \\
&\quad + A_8^{q_1} \left[4C_F \frac{1-2\epsilon}{\epsilon} (-q_{2\perp}^2)^\epsilon \right] + A_8^{q_2} \left[2C_F \frac{2-5\epsilon}{\epsilon} (-q_{2\perp}^2)^\epsilon \right] \left. \right\}. \quad (4.5)
\end{aligned}$$

A. Corrections to Regge vertices

The contribution to the mass operator in the t_1 channel comes from diagrams $A_{2.1}$ and $A_{2.1c}$,

$$A_{2.1} + A_{2.1c} = 2\delta_S^{s.e.} A^{\text{Bom}} = 2\delta_{1Q}^{s.e.1} A^{\text{Bom}}. \quad (4.6)$$

The nonlogarithmic part of diagrams $A_{2.2}$ and $A_{2.2c}$ (the large logarithm $\ln y_2$ is present in the expression for the diagram $A_{2.2}$) contributes to the mass operator in the t_2 channel, resulting in

$$\Re(A_{2.2} + A_{2.2c})|_{(\ln y_2)^0} = 2\delta_{1Q}^{s.e.2} A^{\text{Bom}} = 2\delta_{1\gamma}^{s.e.} A^{\text{Bom}}. \quad (4.7)$$

The sum of the diagrams 3.3X and 3.4X contributes to the correction δ_S^v

$$A_{3.3} + A_{3.3c} + A_{3.4} + A_{3.4c} = A^{\text{Bom}} \delta_S^v. \quad (4.8)$$

The sum of the box-type diagrams in the t_1 channel with large logarithms only has the tree color structure (octet in the t_1 channel) and yields the gluon trajectory

$$(A_{4.1} + A_{4.2} + A_{4.1c} + A_{4.2c})|_{\ln y_1} = A^{\text{Bom}} \omega_g(q_1) \ln y_1. \quad (4.9)$$

In the cross-box color structure the large logarithm $\ln y_1$ vanishes completely (according to the gluon Reggeization).

For the t_2 channel expression, the large logarithm $\ln y_2$ is reduced to the quark trajectory by a more complex way than in the t_1 channel,

$$\begin{aligned}
& (A_{4.3} + A_{4.3c} + A_{4.4} + A_{3.1} + A_{3.2} + A_{3.5} + A_{2.2})|_{\ln y_2} \\
&= A^{\text{Bom}} \omega_q(q_2) \ln y_2. \quad (4.10)
\end{aligned}$$

The squares of the large logarithms $\ln y_2$ vanish in the following sums:

$$(A_{4.3} + A_{4.3c})|_{(\ln y_2)^2} = 0, \quad (A_{4.4} + A_{3.1})|_{(\ln y_2)^2} = 0. \quad (4.11)$$

The following real part of the octet (tree) color structure gives an almost full contribution to the correction to the Regge vertex $\gamma_{R_1 Q_2}^Q$:

$$\begin{aligned}
& \Re(A_{4.3} + A_{4.3c} + A_{4.4} + A_{3.1} + A_{3.1c} \\
&\quad + A_{3.2} + A_{3.2c} + A_5 + A_{4.1} + A_{4.2})|_8 \\
&= A^{\text{Bom}} \left(\omega_g(q_1) \left[\ln y_1 + \frac{1}{2} \ln \frac{k_\perp^2}{q_{1\perp}^2} \right] \right. \\
&\quad + \omega_q(q_2) \left[\ln y_2 + \frac{1}{2} \ln \frac{q_{2\perp}^2}{k_\perp^2} \right] + \delta_{1Q}^{v,c} + \delta_{1\gamma}^A \\
&\quad \left. + \delta_{1\gamma}^c + \delta_S^c + \delta_S^A \right) + A_8^\epsilon \delta_{2Q} + A_8^{q_1} \delta_{2\gamma}^c - A_8^{q_2} \delta_{3\gamma}. \quad (4.12)
\end{aligned}$$

Together with the mass operator contribution (4.6) and (4.7), one obtains the full result for the vertex in question. In the sum (4.12) there are some contributions to the Regge vertices in the fragmentation region, i.e., $\Gamma_{S'S}^R$ [see Eq. (3.7)]

and $\Gamma_{\gamma'Q}^{Q_2}$ [see Eq. (3.11)], and the contributions to the Regge trajectories.

The vertex correction to the photon production vertex comes from the following diagram group and reads

$$\Im(A_{3.5} + A_{3.5c})|_{(\ln y_2)^0} = A^{\text{Bom}}\delta_{1\gamma}^v + A_8^{q_1}\delta_{2\gamma}^v + A_8^{q_2}\delta_{3\gamma}^v. \quad (4.13)$$

It is obvious from expressions (4.12) and (4.13) that the structure of $A_8^{q_2}$ cancels in the final expression for the Regge amplitude.

B. The cross-box color structure and the imaginary part of the amplitude

The cross-box color structure appears only in the diagrams 5X, 4.1X, and 4.2X. We introduce the notation for the basic structure, which is contained in the cross-box color structure,

$$A_{c-b} = -2y_1 g^2 e T_{S_c}^a T_{cS}^b \frac{\bar{u}(k_3) t^b t^a \not{q}_{1\perp} \not{q}_{2\perp} \not{\epsilon}_\perp u(k_5)}{q_{1\perp}^2 q_{2\perp}^2}. \quad (4.14)$$

$$\begin{aligned} i\mathcal{A} = & a_\Gamma g^2 A^{\text{Bom}} \left\{ C_F (-q_{2\perp}^2)^\epsilon \left(-\frac{2}{\epsilon^2} + \frac{3}{\epsilon} - 9 - \frac{2}{\epsilon} \ln y_2 + \frac{2\pi^2}{3} + \frac{3q_{1\perp}^2}{q_{1\perp}^2 - q_{2\perp}^2} \ln \left[\frac{q_{1\perp}^2}{q_{2\perp}^2} \right] \right. \right. \\ & + 2\text{Li}_2 \left[1 - \frac{q_{1\perp}^2}{q_{2\perp}^2} \right] \left. \right\} + N_c (-q_{1\perp}^2)^\epsilon \left(-\frac{2}{\epsilon^2} + \frac{1}{\epsilon} \left(\frac{1}{3} + \frac{4}{9}\epsilon + n_s \left(\frac{1}{6} - \frac{4}{9}\epsilon \right) + \frac{n_f}{N_c} \left(\frac{2}{3} - \frac{10}{9}\epsilon \right) \right. \right. \\ & + \ln \left[\frac{q_{1\perp}^2}{k_\perp^2} \right] - 2 \ln y_1 \left. \right) - \frac{1}{2} \ln^2 \left[\frac{q_{1\perp}^2}{k_\perp^2} \right] + \frac{2\pi^2}{3} - \ln \left[\frac{q_{1\perp}^2}{q_{2\perp}^2} \right] \ln \left[\frac{k_\perp^2}{q_{2\perp}^2} \right] - 2\text{Li}_2 \left[1 - \frac{q_{1\perp}^2}{q_{2\perp}^2} \right] \left. \right\} \\ & + 2C_F a_\Gamma g^2 A_8^{q_1} + a_\Gamma g^2 A_8^e \left\{ (N_c - C_F) \left(1 + \frac{k_\perp^2}{q_{1\perp}^2 - q_{2\perp}^2} - \frac{q_{1\perp}^2 k_\perp^2}{(q_{1\perp}^2 - q_{2\perp}^2)^2} \ln \left[\frac{q_{1\perp}^2}{q_{2\perp}^2} \right] \right) \right. \\ & \left. + C_F \frac{3q_{1\perp}^2}{q_{1\perp}^2 - q_{2\perp}^2} \ln \left[\frac{q_{1\perp}^2}{q_{2\perp}^2} \right] \right\} + i\pi \frac{a_\Gamma g^2}{\epsilon} \{ N_c A^{\text{Bom}} ((-q_{1\perp}^2)^\epsilon + (-k_\perp^2)^\epsilon) - A_{c-b} 4(-q_{1\perp}^2)^\epsilon \}. \quad (4.17) \end{aligned}$$

It is easy to see that the coefficients before the structures $A_8^{q_1}$ and A_8^e are finite in the limit $D \rightarrow 4$.

Comparing the result (4.17) of the amplitude calculation with the expression (3.24) for the real part coming from the Reggeization hypothesis, we can present the effective Regge vertex of the quark production in the central rapidity region in the NLO,

$$\gamma_{R_1 Q_2}^Q = -g \frac{1}{k_3^+} \bar{u}(k_3) t^{R_1} (\not{q}_{1\perp} + \not{q}_{1\perp} \delta_{1Q} + \not{q}_{2\perp} \delta_{2Q}),$$

where

$$\delta_{1Q} = \delta_{1Q}^{s,e,1} + \delta_{1Q}^{s,e,2} + \delta_{1Q}^{v,c}.$$

The cross-box color structure is derived from the amplitude, resulting in

$$\mathcal{A}|_{\text{crossbox}} = g^2 (-ia_\Gamma) A_{c-b} (-i\pi) \frac{4}{\epsilon} (-q_{1\perp}^2)^\epsilon. \quad (4.15)$$

The imaginary part of the amplitude contains tree and cross-box color structures,

$$\Im \mathcal{A} = \pi \frac{(-ia_\Gamma) g^2}{\epsilon} [N_c ((-q_{1\perp}^2)^\epsilon + (-k_\perp^2)^\epsilon) A^{\text{Bom}} - 4(-q_{1\perp}^2)^\epsilon A_{c-b}]. \quad (4.16)$$

It is easy to see that the imaginary part does not contain large logarithms ($\ln y_1$ and $\ln y_2$) at all, as it must be according to the Reggeization hypothesis.

C. The final result for the amplitude and the vertex $\gamma_{R_1 Q_2}^Q$

Now we present the resulting expression for one-loop corrections to the $SQ \rightarrow S'Q'\gamma$ amplitude in the MRK with $\mathcal{O}(\epsilon)$ accuracy:

The contribution from the mass operator has the form

$$\begin{aligned} \delta_{1Q}^{s,e,1} + \delta_{1Q}^{s,e,2} = & \frac{N_c g^2 (-ia_\Gamma)}{2} \left\{ (-q_{1\perp}^2)^\epsilon \left[\frac{n_s}{2} \left(\frac{1}{3\epsilon} - \frac{8}{9} \right) \right. \right. \\ & - \left(\frac{5}{3\epsilon} - \frac{31}{9} \right) + \frac{n_f}{N_c} \left(\frac{4}{3\epsilon} - \frac{20}{9} \right) \left. \right] \\ & \left. + (-q_{2\perp}^2)^\epsilon \frac{C_F}{N_c} \left(\frac{1}{\epsilon} - 1 \right) \right\}. \quad (4.18) \end{aligned}$$

The vertex correction with $\mathcal{O}(\epsilon)$ accuracy acquires the form

$$\begin{aligned}
\delta_{1Q}^{v,c} = g^2(-ia_\Gamma) & \left\{ C_F \left(-\frac{(-k_\perp^2)^\epsilon}{\epsilon^2} + \frac{(-q_{2\perp}^2)^\epsilon}{\epsilon} \right. \right. \\
& + \frac{\pi^2}{6} - 4 + \frac{3q_{1\perp}^2}{q_{1\perp}^2 - q_{2\perp}^2} \ln \left[\frac{q_{1\perp}^2}{q_{2\perp}^2} \right] \Bigg) \\
& + N_c \left(\frac{(-q_{1\perp}^2)^\epsilon}{2\epsilon} + \frac{\pi^2}{6} + 3 - \frac{1}{2} \ln^2 \left[\frac{q_{1\perp}^2}{q_{2\perp}^2} \right] \right) \\
& \left. + (C_F - N_c) \left(\frac{1}{2} \ln^2 \left[\frac{q_{2\perp}^2}{k_\perp^2} \right] + 2\text{Li}_2 \left[1 - \frac{q_{1\perp}^2}{q_{2\perp}^2} \right] \right) \right\}. \tag{4.19}
\end{aligned}$$

The correction to the term violating helicity has the form (which is finite in the limit $\epsilon \rightarrow 0$)

$$\begin{aligned}
\delta_{2Q} = g^2(-ia_\Gamma) & \left\{ (N_c - C_F) \left(1 + \frac{k_\perp^2}{q_{1\perp}^2 - q_{2\perp}^2} \right. \right. \\
& - \frac{q_{1\perp}^2 k_\perp^2}{(q_{1\perp}^2 - q_{2\perp}^2)^2} \ln \left[\frac{q_{1\perp}^2}{q_{2\perp}^2} \right] \Bigg) \\
& \left. + C_F \frac{3q_{1\perp}^2}{q_{1\perp}^2 - q_{2\perp}^2} \ln \left[\frac{q_{1\perp}^2}{q_{2\perp}^2} \right] \right\} + \mathcal{O}(\epsilon). \tag{4.20}
\end{aligned}$$

For the $\mathcal{N} = 4$ SYM case (all particles are in the adjoint color representation) one can obtain a very simple result for the vertex,

$$\begin{aligned}
\gamma_{R_1 Q_2}^{Q(\text{SYM})} = -\frac{g}{k_3^+} \bar{u}(k_3) T_{Q_2}^{R_1} & \left\{ \not{q}_{1\perp} + g^2 N_c (-ia_\Gamma) \right. \\
& \times \left(\not{q}_{1\perp} \left[\frac{3}{2\epsilon} \left((-q_{1\perp}^2)^\epsilon + (-q_{2\perp}^2)^\epsilon \right) \right. \right. \\
& - \frac{(-k_\perp^2)^\epsilon}{\epsilon^2} - \frac{7}{2} + \frac{\pi^2}{3} - \frac{1}{2} \ln^2 \frac{q_{1\perp}^2}{q_{2\perp}^2} \Bigg] \\
& \left. \left. + (\not{q}_{1\perp} + \not{q}_{2\perp}) \frac{3q_{1\perp}^2}{q_{1\perp}^2 - q_{2\perp}^2} \ln \frac{q_{1\perp}^2}{q_{2\perp}^2} \right) \right\}. \tag{4.21}
\end{aligned}$$

Here we have used the following substitutions: $C_F \rightarrow N_c$, $\frac{n_i}{N_c} \rightarrow 4$, $n_s \rightarrow 6 - 2\epsilon$ (in the dimensional reduction scheme).

V. CONCLUSION

Our paper is devoted to the effective vertex $\gamma_{R_1 Q_2}^Q$ calculation in the next-to-leading order. The vertex of

the massless quark Q production in the Reggeon (quark Q_2 and gluon R_1) collision in the t channels was the last unknown NLO vertex in the central rapidity region to formulate the quark Reggeization hypothesis within the next-to-leading-logarithmic approximation. Now all of the components are ready to perform the hypothesis proof using the bootstrap approach [6], which was used in the gluon Reggeization proof in both QCD [9–11] and SYM [12]. The simplicity of the SYM vertex (4.21) gives us an additional tool for the SYM property investigations by use of the multi-Regge amplitude form, as was the case for the gluon Reggeization and Bern-Dixon-Smirnov ansatz [24] in SYM.

In principle, there are some different methods for the effective vertex calculation, with the t -channel unitarity method being the most popular among them. However, in our work we used the straightforward method of the one-loop amplitude calculation equipped with the computer algebra automatization methods based for it on the MATHEMATICA system and LiteRed package [13]. This package was used to reduce integrals emerging in the one-loop amplitude to the basis of master integrals. The master integrals in our problem are of known (massless) pentagon and box types [14]. Our method allows us to perform the cross-check by obtaining other elements of the Regge amplitude (quark and gluon trajectories and known effective vertices) as a byproduct.

ACKNOWLEDGMENTS

This work is supported by the Russian Foundation for Basic Research, Grant No. 13-02-01023, 15-02-07893. A. V. thanks the Dynasty Foundation and the President Program for the financial support. We would like to thank R. N. Lee for helpful comments and discussions.

APPENDIX

1. Integral calculations and notation

We reduce all expressions in Fig. 2 to scalar products and basic helicity structures. There are two vectors that are not included in the denominators of the pentagon diagram type in the amplitude. It means that there will be tensor integrals with up to two indices. There is only one topology of the integral in our problem:

$$\begin{aligned}
J_{12345}(n_1, n_2, n_3, n_4, n_5) = J_{12345}(\vec{n}) & = \int \frac{d^D l}{(2\pi)^D} \frac{1}{D_1^{n_1} D_2^{n_2} D_3^{n_3} D_4^{n_4} D_5^{n_5}}, \\
D_1 = l^2, \quad D_2 = (l + k_1)^2, \quad D_3 = (l + k_1 + k_2)^2, \\
D_4 = (l + k_1 + k_2 + k_3)^2, \quad D_5 = (l + k_1 + k_2 + k_3 + k_4)^2. \tag{A1}
\end{aligned}$$

There are only ten master integrals in this topology that have the form $J_{12345}(\vec{n}_i)$, $i = 1, \dots, 10$, where \vec{n}_i are of the form

$$\begin{aligned} \vec{n}_1 &= (1, 1, 1, 1, 1), & \vec{n}_2 &= (1, 1, 1, 1, 0), & \vec{n}_3 &= (1, 1, 1, 0, 1), & \vec{n}_4 &= (1, 1, 0, 1, 1), & \vec{n}_5 &= (1, 0, 1, 1, 1), \\ \vec{n}_6 &= (1, 0, 1, 0, 0), & \vec{n}_7 &= (1, 0, 0, 1, 0), & \vec{n}_8 &= (0, 1, 0, 1, 0), & \vec{n}_9 &= (0, 1, 0, 0, 1), & \vec{n}_{10} &= (0, 0, 1, 0, 1), \end{aligned}$$

and one has four integral types with the same topology which have different permutations of the external momenta:

	D_1	D_2	D_3	D_4	D_5
J_{12345}	l^2	$(l+k_1)^2$	$(l+k_1+k_2)^2$	$(l+k_1+k_2+k_3)^2$	$(l+k_1+k_2+k_3+k_4)^2$
J_{21345}	l^2	$(l+k_2)^2$	$(l+k_1+k_2)^2$	$(l+k_1+k_2+k_3)^2$	$(l+k_1+k_2+k_3+k_4)^2$
J_{12435}	l^2	$(l+k_1)^2$	$(l+k_1+k_2)^2$	$(l+k_1+k_2+k_4)^2$	$(l+k_1+k_2+k_3+k_4)^2$
J_{41235}	l^2	$(l+k_4)^2$	$(l+k_1+k_4)^2$	$(l+k_1+k_2+k_4)^2$	$(l+k_1+k_2+k_3+k_4)^2$

There are only three different types of master integrals. The first one is a pentagon with massless external lines [for example, $J_{12345}(\vec{n}_1)$]. The second one is a box with one external line with mass [for example, $J_{12345}(\vec{n}_2)$]. And the third type is a bubble [for example, $J_{12345}(\vec{n}_6)$].

The following table shows the integrals used in the diagrams in Fig. 2.

Integrals	Diagrams
J_{12345}	$d5, d4.1, d4.2, d4.4, d3.X, d2.X$
J_{21345}	$d5c, d4.1c, d4.2c$
J_{12435}	$d4.3$
J_{41235}	$d4.3c$

2. Tensor momentum integrals

We introduce the following notation $I[\cdot]$ for various integrands containing the argument of the square bracket in the numerator with l being the loop momentum. For instance,

$$I[l^\mu] \equiv \int \frac{d^D l}{(2\pi)^D} \frac{l^\mu}{D_1^{n_1} D_2^{n_2} D_3^{n_3} D_4^{n_4} D_5^{n_5}}. \quad (A2)$$

An integral with an external index μ is expressed as a linear combination of the incoming momenta:

$$I[l^\mu] = \sum_i k_i^\mu I[a_i], \quad (A3)$$

where a_i are scalar polynomial functions of l^μ . It is easy to express the integral with an external index as a linear combination of integrals without external indices. Since we have four independent vectors k_i (that are in the four-dimensional subspace), the matrix m_{ij} is invertible. It is easy to find that eventually

$$I[l^\mu] = \sum_{ij} k_i^\mu m_{ij}^{-1} I[k_j \cdot l], \quad k_i \cdot k_j = m_{ij}, \quad (A4)$$

where $I[k_j \cdot l]$ can be expressed in terms of integrals with other powers of denominators.

The tensor integral with two indices can be expressed through the metric tensor subspace $D-4$ and through momenta entering the integral:

$$\begin{aligned} I[l^\mu l^\nu] &= g_{D-4}^{\mu\nu} I[A] + \sum_{i,j,r,n} m_{ij}^{-1} m_{rn}^{-1} k_i^\mu k_r^\nu I[(k_j \cdot l)(k_n \cdot l)], \\ g_{D-4}^{\mu\nu} k_{i\mu} &= 0, \quad g_{D-4}^{\mu\nu} g_{\mu\nu} = D-4. \end{aligned} \quad (A5)$$

The coefficient before the metric tensor can be easily calculated:

$$I[A] = \frac{1}{D-4} \left(I[l^2] - \sum_{ij} m_{ij}^{-1} I[(l \cdot k_i)(l \cdot k_j)] \right), \quad (A6)$$

$$\begin{aligned} I[l^\mu l^\nu] &= \frac{g^{\mu\nu} - m_{ij}^{-1} k_i^\mu k_j^\nu}{D-4} (I[l^2] - m_{rn}^{-1} I[(l \cdot k_r)(l \cdot k_n)]) \\ &\quad + m_{ij}^{-1} m_{rn}^{-1} k_i^\mu k_r^\nu I[(k_j \cdot l)(k_n \cdot l)]. \end{aligned} \quad (A7)$$

The integrals with three external Lorentz indices will not arise in our problem. A loop momentum convoluted with the momentum included in the denominator is easily expressed in terms of a linear combination of the denominators. In our calculation integrals with two indices appear only in the expression of $I[(e \cdot l)I]$.

3. Master integrals

We work in the dimensional regularization with $D = 4 + 2\epsilon$. Hereafter we use the notation for the common multiplier emerging in integral calculations,

$$a_\Gamma = i \frac{\Gamma(3 - \frac{D}{2}) \Gamma^2(\frac{D}{2} - 1)}{(4\pi)^{\frac{D}{2}} \Gamma(D-3)}. \quad (A8)$$

In the master integral expressions [14] we assume all the invariants to be negative. To analytically continue these expressions to the physical region of our process (see Fig. 1) it is necessary to make a prescription $(k_i + k_j)^2 = s_{ij} \rightarrow s_{ij} + i0$ for the invariants involved.

There are three principal master integrals in our calculation [14]:

$$\begin{aligned}
J_{12345}(1, 0, 1, 0, 0) &= \int \frac{d^D l}{(2\pi)^D} \frac{1}{l^2(l+k_1+k_2)^2} = -a_\Gamma \frac{(-t_1)^\epsilon}{\epsilon(1+2\epsilon)}, \quad t_1 < 0; \\
J_{12345}(1, 1, 1, 1, 0) &= \int \frac{d^D l}{(2\pi)^D} \frac{1}{l^2(l+k_1)^2(l+k_1+k_2)^2(l+k_1+k_2+k_3)^2} \\
&= 2a_\Gamma \frac{(-t_2)^{-\epsilon}}{(-t_1)^{1-\epsilon}(-s_1)^{1-\epsilon}} \left[\frac{1}{\epsilon^2} + \text{Li}_2\left(1 - \frac{t_1}{t_2}\right) + \text{Li}_2\left(1 - \frac{s_1}{t_2}\right) - \frac{\pi^2}{6} \right] + \mathcal{O}(\epsilon), \\
& \quad s_1 < 0, \quad t_1 < 0, \quad t_2 < 0; \\
J_{12345}(1, 1, 1, 1, 1) &= \int \frac{d^D l}{(2\pi)^D} \frac{1}{l^2(l+k_1)^2(l+k_1+k_2)^2(l+k_1+k_2+k_3)^2(l+k_1+k_2+k_3+k_4)^2} = \\
& - a_\Gamma \left\{ \frac{(-s)^{-\epsilon}(-t_1)^{-\epsilon}}{(-s_1)^{1-\epsilon}(-s_2)^{1-\epsilon}(-t_2)^{1-\epsilon}} \left(\frac{1}{\epsilon^2} + 2\text{Li}_2\left(1 - \frac{s_1}{s}\right) + 2\text{Li}_2\left(1 - \frac{t_2}{t_1}\right) - \frac{\pi^2}{6} \right) \right. \\
& + \frac{(-t_1)^{-\epsilon}(-s_1)^{-\epsilon}}{(-s_2)^{1-\epsilon}(-t_2)^{1-\epsilon}(-s)^{1-\epsilon}} \left(\frac{1}{\epsilon^2} + 2\text{Li}_2\left(1 - \frac{s_2}{t_1}\right) + 2\text{Li}_2\left(1 - \frac{s}{s_1}\right) - \frac{\pi^2}{6} \right) \\
& + \frac{(-s_1)^{-\epsilon}(-s_2)^{-\epsilon}}{(-t_2)^{1-\epsilon}(-s)^{1-\epsilon}(-t_1)^{1-\epsilon}} \left(\frac{1}{\epsilon^2} + 2\text{Li}_2\left(1 - \frac{t_2}{s_1}\right) + 2\text{Li}_2\left(1 - \frac{t_1}{s_2}\right) - \frac{\pi^2}{6} \right) \\
& + \frac{(-s_2)^{-\epsilon}(-t_2)^{-\epsilon}}{(-s)^{1-\epsilon}(-t_1)^{1-\epsilon}(-s_1)^{1-\epsilon}} \left(\frac{1}{\epsilon^2} + 2\text{Li}_2\left(1 - \frac{s}{s_2}\right) + 2\text{Li}_2\left(1 - \frac{s_1}{t_2}\right) - \frac{\pi^2}{6} \right) \\
& \left. + \frac{(-t_2)^{-\epsilon}(-s)^{-\epsilon}}{(-t_1)^{1-\epsilon}(-s_1)^{1-\epsilon}(-s_2)^{1-\epsilon}} \left(\frac{1}{\epsilon^2} + 2\text{Li}_2\left(1 - \frac{t_1}{t_2}\right) + 2\text{Li}_2\left(1 - \frac{s_2}{s}\right) - \frac{\pi^2}{6} \right) \right\} + \mathcal{O}(\epsilon), \\
& \quad s < 0, \quad s_1 < 0, \quad s_2 < 0, \quad t_1 < 0, \quad t_2 < 0;
\end{aligned}$$

Here we use the notations (2.1) for kinematic invariants.

In the analytical continuation to the physical domain in polylogarithmic functions, one needs to choose the correct branch using the following properties:

$$\text{Li}_2(x \pm i0) = \frac{\pi^2}{3} - \frac{1}{2} \ln^2 x - \text{Li}_2(x^{-1}) \pm i\pi \ln x, \quad x > 1.$$

Given that σ_1, σ_2 are the signs of s_1, s_2 , for the case $\sigma_1\sigma_2 = -1$ one has

$$\text{Li}_2\left(1 - \frac{s_1 + i0}{s_2 + i0}\right) = \frac{\pi^2}{3} - \frac{1}{2} \ln^2\left(1 - \frac{s_1}{s_2}\right) - \text{Li}_2\left(\frac{1}{1 - \frac{s_1}{s_2}}\right) + i\sigma_1\pi \ln\left(1 - \frac{s_1}{s_2}\right).$$

-
- | | |
|--|--|
| [1] I. I. Balitsky and L. N. Lipatov, <i>Yad. Fiz.</i> 28 , 1597 (1978) [<i>Sov. J. Nucl. Phys.</i> 28 , 822 (1978)]. | [8] V. S. Fadin, M. G. Kozlov, and A. V. Reznichenko, <i>Yad. Fiz.</i> 67 , 377 (2004) [<i>Phys. At. Nucl.</i> 67 , 359 (2004)]. |
| [2] V. S. Fadin, E. A. Kuraev, and L. N. Lipatov, <i>Phys. Lett.</i> 60B , 50 (1975). | [9] V. S. Fadin, M. G. Kozlov, and A. V. Reznichenko, <i>Phys. At. Nucl.</i> 74 , 758 (2011). |
| [3] E. A. Kuraev, L. N. Lipatov, and V. S. Fadin, <i>Zh. Eksp. Teor. Fiz.</i> 71 , 840 (1976) [<i>Sov. Phys. JETP</i> 44 , 443 (1976)]. | [10] V. S. Fadin, M. G. Kozlov, and A. V. Reznichenko, <i>Phys. At. Nucl.</i> 75 , 850 (2012). |
| [4] E. A. Kuraev, L. N. Lipatov, and V. S. Fadin, <i>Zh. Eksp. Teor. Fiz.</i> 72 , 377 (1977) [<i>Sov. Phys. JETP</i> 45 , 199 (1977)]. | [11] V. S. Fadin, M. G. Kozlov, and A. V. Reznichenko, <i>Phys. At. Nucl.</i> 75 , 493 (2012). |
| [5] L. N. Lipatov, <i>Sov. J. Nucl. Phys.</i> 23 , 338 (1976). | [12] V. S. Fadin, M. G. Kozlov, and A. V. Reznichenko, <i>Phys. At. Nucl.</i> 77 , 251 (2014). |
| [6] V. S. Fadin, R. Fiore, M. G. Kozlov, and A. V. Reznichenko, <i>Phys. Lett. B</i> 639 , 74 (2006). | [13] R. N. Lee, <i>J. Phys. Conf. Ser.</i> 523 , 012059 (2014), http://www.inp.nsk.su/~lee/programs/LiteRed/ . |
| [7] A. V. Bogdan and V. S. Fadin, <i>Nucl. Phys.</i> B740 , 36 (2006). | |

- [14] Z. Bern, L. Dixon, and D. Kosower, *Nucl. Phys.* **B412**, 751 (1994).
- [15] V. S. Fadin and R. Fiore, *Phys. Rev. D* **64**, 114012 (2001).
- [16] L. N. Lipatov and M. I. Vyazovsky, *Nucl. Phys.* **B597**, 399 (2001).
- [17] V. S. Fadin, *Phys. At. Nucl.* **66**, 2017 (2003).
- [18] A. V. Bogdan and A. V. Grabovsky, *Nucl. Phys.* **B773**, 65 (2007).
- [19] V. S. Fadin and L. N. Lipatov, *Nucl. Phys.* **B406**, 259 (1993).
- [20] V. S. Fadin, R. Fiore, and A. Papa, *Phys. Rev. D* **63**, 034001 (2000).
- [21] V. Del Duca and C. R. Schmidt, *Phys. Rev. D* **59**, 074004 (1999).
- [22] R. E. Gerasimov and V. S. Fadin, *Phys. At. Nucl.* **73**, 1214 (2010).
- [23] A. V. Bogdan and A. V. Grabovsky, *Nucl. Phys.* **B757**, 211 (2006).
- [24] Z. Bern, L. J. Dixon, and V. A. Smirnov, *Phys. Rev. D* **72**, 085001 (2005).